Stony Brook University

CERAMIC NANOMATERIALS FOR ENERGY

A Thesis Presented

By

Gagan Jodhani

To

The Graduate School

In Partial Fulfillment of the Requirements

For the Degree of

Master of Science

In

Materials Science and Engineering

Stony Brook University

December 2010

Stony Brook University

The Graduate School

Gagan Jodhani

We, the thesis committee for the above candidate for the

Master of Science degree, hereby recommend

acceptance of this thesis.

Pelagia Irene (Perena) Gouma - Advisor
Associate Professor Department of Materials Science and Engineering

Jonathan C Sokolov
Professor Department of Materials Science and Engineering

Charles M Fortman
Associate Professor Department of Materials Science and Engineering

This thesis is accepted by the Graduate School

Lawrence Martin
Dean of the Graduate School

Abstract of the Thesis

CERAMIC NANOMATERIALS FOR ENERGY

By

Gagan Jodhani

Master of Science

In

Materials Science and Engineering

Stony Brook University

2010

In this work we try to synthesize MoO_3 and WO_3 nanoceramics by understanding the effects of precursor parameters on the electrospinning process. We synthesized polymer based composites with molybdenum oxide and Tungsten oxide under straight polarity i.e. keeping needle charged and collector grounded; as well as reverse polarity i.e. keeping the needle grounded and collector charged. We observed MoO_3 nanotubes after heat treatment of the composite mats spun in reverse polarity. The reason for formation of nanotubes is the presensce of molybdenum oxide particles as an outer shell surrounding the polymer fiber core in the spun mats, this core shell configuration can be correlated with the zeta potential of the sol gel that is electronegative; and thus the sol forms a shell around the polymer when the collector is positively charged. For WO_3, we obtained a nanogrid structure after thermal treatment under both conditions (straight and reverse polarity). The reason for the formation of the grids is due to the immiscibility of the metal oxide particles in colloid solution. The nanostructures obtained for MoO_3 and WO_3 are very promising candidates to be used as solar cells, photocatalysts or as negative electrodes in Li-ion batteries.

Table of Contents

List of Figures

List of Tables

ACKNOWLEDGEMENT

I would like to thank my advisor Professor Perena Gouma; for her guidance and help with my research. I also thank Professor Jonathan Sokolov and Professor Charles Fortman for being on my thesis committee. I also thank Professor Gary Halada for allowing me to carry FTIR experiments in his lab.I wish to thank Mike Cuiffo for helping me carry out FTIR spectroscopy on my samples. I also thank Dr. Krithika Kalyanasundaram for her guidance. I would also like to thank Dr. Jim Quinn for his help with the SEM experiments. I would like to extend my thanks to my group members Ruipeng, Jusang and Andrea. Finally, I thank my family and my friends for their support at all times.

Chapter 1

Introduction

Energy is an important factor in our day to day life. Most of our energy needs are dependent on fossil fuels. Since there is a limited amount of fossils available and increasing demands for it, scientists worldwide have been working on renewable sources of energy. Solar Energy has been a first choice as it is free and readily available. Solar cookers for food preparation, solar water heater etc are being used since a quite a long time now. Solar Cells have also been developed and are applied for production of electricity for small needs. Solar cells utilizes Also Lithium ion batteries, are being used for powering electronic devices such as cell phones, laptops etc. Scientists have also been researching on fuel cells that can be used to for automobiles, generation of electricity etc.

Metal oxides play an important role in the manufacturing of these devices as apart for their potential to be used in batteries, solar cells and fuels cells, metal oxides are much cheaper than the materials that were initially used for these purposes. However, in some cases it has been noticed that with the replacement of conventional materials with metal oxides the overall efficiency decreases. Still metal oxides are considered for such applications due to their low cost: performance ratio.

Another advantage of metal oxide lies in the fact that they can be made in the form of nanowires, nanospheres, nanorods, nanotubes etc. The application of nanotechnology has revolutionized the field, as nanostructured materials offer greater surface area and hence are more efficient.

1.1 Methods of Fabrication

1.1.1 Sol Gel Synthesis:

A sol gel is a colloidal suspension of solid particles in liquid. Sol gel processing is a technique to prepare a sol, its gelation, and removal of solvent [1]. The gel obtained consists of a continuous solid phase in a continuous liquid phase. The sol can be produced from either an organic or inorganic precursor. A precursor is an initial compound required to process the sol gel. The precursors readily react with water to give metal based sol gels. Metal alkoxides are

used as a precursor for metal based sol gels. Alkoxides have a organic ligand attached to the metal atom. The organic ligand reacts with water and giver metal hydroxide and alcohol. The equation for this is given by:

$$M\text{-}(O\text{-}R)_x + xH_2O \rightarrow M\text{-}(O\text{-}H)_5 + xR\text{-}O\text{-}H$$

Where R is the alkyl group attached to the precursor.

After the formation of sol gel, there are number of ways in which metal oxides can be derived from them in the desired form. Thin films can be obtained by spin coating and then thermally treating the material in order to achieve phase change.

1.1.2 Electrospinning: Principles and Operation

Electrospinning was first patented by Formhals in 1934 for textile weaving[2]. A typical electrospinning setup consists of a syringe pump, a syringe with needle, a grounded collector and a high voltage power supply. The solution that is to be spun is filled in the syringe; the syringe is then loaded on the syringe pump which pumps the solution at a very low rate. The needle of the syringe is connected to the high voltage power supply, either a positive or a negative potential can be used. The collector is grounded, due to high potential difference developed in between the needle and the collector the fibers get deposited on the collector.

The setup for electrospinning is very easy, but the science involved in making of the nanofibers is relatively very complex. There are too many parameters that affect the morphology of the spun nanofibers. The various parameters that affect electrospun nanofibers are potential applied across the needle, viscosity of the solution, concentration of the solution, distance between the needle and the collector, conductivity of the solution, feed rate, internal diameter of the needle etc.

For electrospinnig surface tension plays an important role. The charge on the solution should be high enough to overcome the surface tension. A high surface tension may lead to breakup of solution into droplets. For a pure liquid a droplet will acquire a shape that has lowest surface area to volume ratio. In case of solvent mixtures it is more complex; as the composition at surface is often different than bulk [3]. A high surface tension could also lead to formation of beads in the fiber, as the high surface tension tends to stabilize the drops by forming a spherical structure [4]. When the electrostatic force is large enough to counteract the surface tension, the solution is extended. At a significant point a stream of liquid erupts from the surface. The

extended solution is in the form of a cone, which is known as taylor cone. The formation of taylor cone corresponds to a specific self similar solution, this formation is dependent on a certain critical level of electric field [5].

Viscosity of a solution also has a deep effect on electrospinning and resultant fiber morphology. For electrospinning to occur, jet stabilization is required. To achieve this; a sufficiently high extensional viscosity is required [6].

Electrospinning could be applied to obtain core-shell fibers. Bazilevsky et al. demonstrated a co-electrospinning technique to obtain core-shell nanofibers for poly(methyl methacrylate)(PMMA)/polyacrylonitrile (PAN)solutions in dimethylformamide [7]. The process relied on precipitation of PMMA solution droplets which, became trapped at the base of taylor cone; stretching of which resulted in core shell fibers. Kameoka J. et al. developed a scanning tip electrospinning source for deposition of oriented fibers, the process yielded fibers of uniform diameter [8]. However, the disadvantage of this process is that it is not continuous.

Apart from non woven mat it is also possible to obtain uniformly aligned fibers through electrospinning. The technique used for the process is that a rotating cylindrical collector is used to collect the fibers. The rotation of collector leads to the stretching of fibers and get aligned in a uniform way. Jalili R et al. designed a process to obtain uniformly aligned nanofibers by using two electrically conducting plates as collector separated by an insulating gap. The fiber was deposited on the conducting plates and was stretched in the non conducting region giving rise to uniformly aligned fibers [9].

Thus it can be said that by controlling the parameters of the electrospinning process it is possible to obtain desired morphology for the nanofibers.

1.2 MATERIALS FOR ENERGY

Metal oxide ceramics have been used for various energy applications. It is not possible to discuss all of them together under a same title as different devices require different characteristics of these ceramics; hence they have been discussed individually below.

1.2.1 Li-ion Batteries

Rechargeable batteries have always been a good power source for a wide variety of applications due to the face that they are light weight, rechargeable and cost effective. Currently almost all electronic portable devices are running on Li-ion batteries.

A typical Li-ion battery consists of a cathode, an anode and an electrolyte for charge transport. A lot of research is being carried on to increase the capacity and recharging rates of these batteries. This is where metal oxides come in handy. It has been shown that transition metal oxides as negative electrodes are better than the conventional graphite electrodes used in Li-ion batteries as they demonstrate higher electrochemical capacity [10]. Oxides of transition metals such as Fe, Ni, Co, Mn, Sb, Sn etc. Nanostructured metal oxides are good choice for the anodes as they provide large surface area, also their porous nature enhances the diffusion of Li^+ ions which in turn yields in higher charge capacity. However, there exists some problems with metal oxides; they have low charge retention i.e. the charge capacity tends to decrease with more number of cycles and chances of structural transition. These drawbacks in some materials can be avoided by carbon coatings the nanomaterial[11] or doping[12] with another metal. Table 1.1 shows the charge capacity of different metal oxide nanomaterials and lists their advantages over conventional graphite electrodes. Though these materials have a high capacity and charge retention also there exists a certain drawback with them. The major drawback of most of these materials is they require a lengthy procedure for the preparation of anodes and the process is not feasible for industrial applications. V_2O_5 has also been tested as a potential material for rechargeable batteries [13], but they yielded poor cycling performance and low cycling capacity. These drawbacks of V_2O_5 can be avoided by using $FeVO_4.0.92H_2O$ or $Sn_2VO_6.0.78H_2O$ as they have high initial capacities (>1650 mAh g^{-1}) and better cycling performances.

The conventional electrodes used the principle of intercalation of lithium ions. Both anodes and cathodes can transport lithium ions. During the discharging of battery, the current flow is regulated by flow of Li^+ ions from anode to cathode through the electrolyte[17]. During the availability of external power source the Li^+ ions travel in reverse direction. Metal oxides when used as electrodes use different mechanism. For Li-ion batteries with metal oxides as cathodes, during the discharging process oxidation Li ions travel from anode to cathode through the electrolyte and Li_2O is formed[18]. When external power is applied, Li_2O decomposes and Li ions move in reverse direction. Since in both cases the reactions takes place at the electrodes, morphology of the material that offers more surface area for reaction can yield better current density.

Table 1.1: Metal oxides for application as anode in Li-ion batteries

Material	Dopant	Morphology	Charge Capacity(m A h g^{-1})	Advantages	Ref.
Fe_3O_4-C*	-	Nanospindles	530	1. Stabilized SEI films 2. High specific capacity 3. High electronic conductivity	11
α-MnO_2	Se	Nanowires	-	1. Doping increases electrode performance. 2. Structural transition is avoided due to doping.	12
SnO_2-C**	-	Nanowires	460	1. Good charge retention 2. Cyclic retention achieved	22
γ-MnO_2	-	Carambola like thin films	500	1. Exhibits high potential plateau. 2. Can be applied in capacitors	23
Sb_2O_3	-	Nanostructured thin film	794	1. High charge capacity 2. Reduces the resistance of active material	24
Co_3O_4	-	nanowires	700	1. High capacity and rate capability	25
CuO	-	nanofibers	560	1. High rate capability and good cyclability 2. Doesn't require a polymer binder	26
Cu_2O	-	Thin film	219	1. Good cyclability	27

*carbon coated, SEI: Solid electrolyte interphase, **carbon encapsulated

Transition metals have also been used as a dopant on the cathode in Li-ion batteries. These electrodes are made as nanostructured Lithium Transition metal oxides and are low in cost, have high energy density and excellent cycle life than Lithium electrodes. Some of the examples of such materials are $LiCoO_2$[14], $LixNiO_2$[15], $LiMn_2O_4$[16] etc. Sometimes the oxides have also been doped with metals to improve their behavior. $LiAl_yCo_{1-y}O_2$[17] is such an example where doping with Al increased the equilibrium voltage relative to $LiCoO_2$. Many of the transition metal oxides are also used as coatings on cathodes to obtain better stability[18]. TiO_2 has been a prime choice for this purpose as they show good Lithium storage properties[19-21].

1.2.2 Solar Cells

Solar cells are efficient devices that convert sunlight into electricity. The generation of electricity from sunlight is due to photovoltaic effect i.e. the material generates a voltage on exposure to electro-magnetic radiation. Many of the solar cells use silicon wafers for conversion of light into electricity. However, these cells are very expensive which led to the search for new

materials for solar cells. Grätzel[28] in 1991 introduced the concept of dye sensitized solar cells(DSSC). These cells used thin film TiO_2 as anode and a charge-transfer dye to sensitize the film for light harvesting. The mechanism of these DSSC is that when a photon is absorbed by the dye molecule, it leads to an electron injection in the conduction band of semiconductor. To complete the circuit the electron transfer from semiconductor material to a carbon counter electrode, the dye is regenerated by electron transfer through an electrolyte (redox species). Although it has a lower conversion efficiency compared to conventional thin film silicon solar cells, its low cost made it feasible for practical applications.

Table 1.2 Metal oxides for DSSC

Material	morphology	Substrate	V_{OC}(mV)	J_{SC}(mA/cm^2)	FF	Ref.
ZnO/poly (vinyl acetate)	Nanofibers	Glass/SnO_2	600	3.58	0.62	29
ZnO/poly-3-hexylthiophene	nanorods	Glass/ indium tin oxide	-	2.0	-	30
ZnO	Tetrapods	Glass/tin oxide	-	-	-	33
ZnO/poly-3-hexylthiophene heated at 150°C	nanorods	-	438	1.24	0.47	31
TiO_2/F8T2*	-	Glass/indium tin oxide	800	0.3	0.25	35
Phosphorous stabilized TiO_2	Mesoporous film	F-doped SnO_2 glass	-	-	-	36

*F8T2:poly(9,9'- dioctylfluorene-co-bithiophene)

Since the introduction of the concept of DSSC researchers have been working on new materials and dyes to improve its overall quality. Apart from TiO_2, ZnO[29-33] is the material that has attracted many scientists as a material for DSSC. ZnO although it has shown lower efficiencies compared to TiO_2 still can be used for practical applications with appropriate dye. Ruthenium based complexes[33-34] are mostly used as charge-transfer dyes as it has been shown that they offer good stability to DSSCs.

The processing parameters also affect the overall performance of the films. It has been shown for ZnO[31] that nanorods treated at 150℃ have better open circuit voltage(V_{OC}), short circuit current density(J_{SC}) and fill factor(FF) than those treated by UV/Ozone.

1.2.3 Fuel Cells

A fuel cell is an electrochemical device that generates electricity through reaction between a fuel and an oxidant, which is triggered by an electrolyte. The first application of fuel cells is reported in space technologies [37]. It was a device which can provide electricity, heat and potable water, which was more convenient than other power sources. Since then it has been considered as an efficient replacement for fossil fuels for generation of energy. Researchers are working on to further develop materials and design [38-40] that enhances the performance of fuel cells.

The basic design of a fuel cell contains an anode and a cathode separated by an electrolyte. The function of the anode, cathode and the electrolyte varies with the type of fuel cell they are used in.

Solid oxide fuel cells (SOFC) use metal oxides as electrolyte. The operation temperature of SOFC is usually high (>500℃). The function of electrolyte is to transport the oxygen and act as a barrier to electrons. The mechanism of SOFC is that the cathode converts oxygen from preheated air into ions which are then transported to the anode via migration through the ceramic electrolyte. At the anode the oxygen ions react with hydrogen fuel and oxygen ions to give electrons which leads to production of electricity, water and since reaction is exothermic heat is generated. Unlike batteries and solar cells, fuel cells have to be provided with fuel which gets consumed in the generation of energy. It is still a better choice than fossils as the fuel does not give any harmful byproducts and requires less chemical processing.

The traditional SOFC was made with yttria based zirconia(YSZ) as electrolyte, nickel-YSZ cermets as anode and Lanthanum strontium magnetite as a cathode[41]. The operating temperature for this fuel cell was 1000℃. Materials have been studied by varying the dopant in these conventional electrodes and electrolyte. Anbin yu et al[42] studied Mg doped $LaCoO_3$ as a potential material for cathode in fuel cells. The results yielded that doping led to a drop in activation energy and oxidation/reduction energy. Metal oxides also find a wide application as fuel cell catalyst support material. Table 1.3 lists the various materials and their applications in SOFC. Apart from SOFC, metal oxides have also been used in other fuel cell types, such as TiO_2 has potential to be used as a catalyst in polymer electrolyte fuel cells[43] (PEFC), SnO_2 when doped with Sb[44] can be used as a catalyst for methanol fuel cells, etc.

Table 1.3: Fuel cell materials for SOFC

Material	Dopant	Application	Ref.
$LaCoO_3$	Mg	Fuel cell cathode	42
SFC1 and SFC2(Sr-Fe -Co system)	-	Fuel cell cathode	45
$Gd_2Zr_2O_7$	-	Fuel cell electrolyte	46
$LaGaO_3$	Co	Fuel cell electrolyte	47
$SrTiO_3$	Nb	Fuel cell anode	48

1.3 Role of nanostructures

Nanomaterials are materials with either one of their dimension less than 100nm. Nanomaterials can be made in the form of rods, spheres, tubes, wires etc. Applications of nanosized materials have a lot of advantages over its micro counterparts in the field of energy. First, they offer a high surface area that increases electronic conductivity. Second, they optimize the rate of transport of electron, proton and reactants in fuel cells[49]. Third, they coordinate mass transport and charge transport in batteries, which is necessary for storage and release of energy. Also, nanomaterials can be tailored to suit the need thus compensating the limitations of the material. Nanostructured SnO_2-TiO_2[50] have shown lower irreversibility compared to macro crystalline SnO_2. Agglomeration of nanosized materials[51] yielded in homogeneous porosity and a narrow pore size distribution which offer a potential for boosting the performance of batteries. Perovskite phases when made in the form of nanotube[52] for use as catalyst prevented high surface area material from corrosion.

Thus it can be said that nanostructure plays an important role in improving surface and electronic properties of metal oxides. High performance devices with greater efficiency can be manufactured with the application of nanostructured materials.

Chapter 2

Experimental Methods

2.1 Sol Gel Synthesis

Molybdenum isopropoxide and tungsten isopropoxide were obtained through Alfa Aesar; they are the precursors for obtaining MoO_3 and WO_3 respectively. The precursors were obtained in 5% wt/volume in isopropanol. The sol gels for the solutions were made by adding water to them. The hydrolysis was done in a glove box in a controlled atmosphere and the resulting solution was mechanically agitated inside the glove box for 5 minutes. The solution was then ultrasonicated for 2 hours and the aged for 24 hours; to ensure complete hydrolysis of the solution.

The hydrolysis of the solution resulted in metal hydroxide dissolved in isopropanol. The metal hydroxide sols were then mixed with PVP solution indifferent ratios to obtain a solution for electrospinning nanocomposites.

2.2 Electrospinning Setup

The electrospinning setup consists of a syringe pump, a needle, a grounded collector and a high voltage power supply. The syringe pump used was from KdScientific, It was a horizontal electrospinning setup. The flow rate for the pump could be calibrated from 0.1µl/min to 153.1µl/min. The High Voltage Power Supply used was from Gamma High Voltage Research and was capable of generating potential from 0-+30KV. A metallic plate covered with aluminum foil was used as a collector. The aluminum foil was used to ensure conductivity and in order to obtain all the nanofibers from the collector. Figure 2.1 shows an electrospinning setup.

For Straight Polarity Electrospinning, The needle was connected to the High Voltage Power Supply and the Collector was grounded, For the Reverse Polarity Electrospinning the needle was grounded and the collector was connected to the Power supply. The flow rate, Potential and the distance between the needle and the collector were kept constant for all the experiments. Figure 2.1 shows the setup for electrospinning.

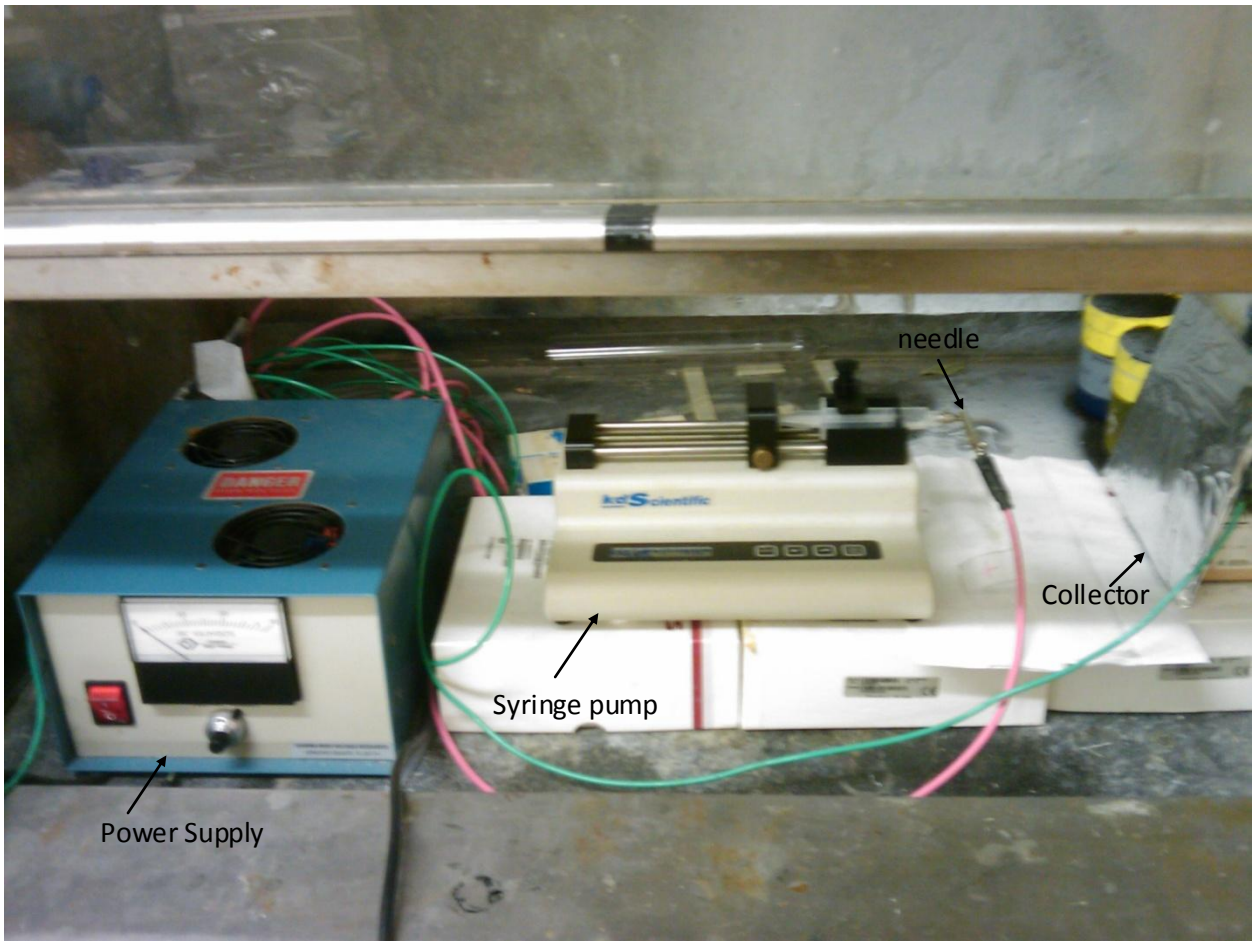

Figure 2.1 Electrospinning Setup

For Electrospinning nanocomposites, sol gel and polymer solution were used. The sol gel synthesis is explained in section 2.1. The precursor polymer used was PVP (Polyvinylpyrrolidone- MW 1,300,000 obtained from Sigma Aldrich). The polymer was dissolved in ethanol to obtain a .1mM solution. .1 mM was chosen because it was observed that below this concentration the polymer wasn't viscous enough to form fibers for the parameters being used. The polymer solution was then mixed with the molybdenum and tungsten sol gels in the ratios of 4:1, 3:1 and 3:2. The final solutions were then fed into a syringe and the nanofibers were obtained under both straight and reverse polarity.

2.3 Characterization

2.3.1 Scanning Electron Microscopy

In order to obtain the morphology of the Polymer + Metal Sol gel nanocomposites, Scanning Electron Microscopy (SEM) was carried out on a LEO-1550 Field Emission Gun SEM. Gold Particles were deposited on the as spun nanofibers via sputtering to ensure conductivity. The images obtained for the as spun fibers and the thermally treated nanoceramics were used to analyze the behavior of the sol gel + polymer solution when subjected to different polarity.

2.3.2 Zeta Potential

Zeta potential can be defined as measure of electrokinetic potential in colloidal system. The particles present in a solution carry a charge at their surface. The sign of zeta potential describes the charge they carry. Aqueous solutions for all colloids are electronegative; i.e. the aqueous suspensions of low ionic concentration in the 5-10 pH range. A low value of zeta potential (-5 - +5 mV) represents agglomeration, higher zeta potential shows stability in the solution [53].

Brookhaven Instruments' ZetaPlus Zeta Potential Analyzer was used to measure Zeta Potential. The technique applied in the instrument is electrophoretic light scattering; which is based on reference beam optics and a dip-in electrode system [54]. The concept used in calculating Zeta potential is that an electric field is applied in the liquid; the charged particles dispersed in a liquid will move towards either the positive or negative pole of the applied field. The direction a particle selects indicates the charge it carries. The velocity which they translate is equivalent to the magnitude of the charge they carry.

Knowing the zeta potential of a solution or a mixture can help in understanding the behavior of the solution in electrospinning jet. The charge the particles carry will allow us to understand how they will behave when a high potential is applied.

2.3.3 FTIR Spectroscopy

A Nicolet Model Magna 760 FTIR spectrometer with a Thermo Spectra-Tech Infinity Reflachromat 32X lens was used for analysis. Readings were taken by placing the nanofibers on a gold plated slide and background readings were subtracted from it. A $4cm^{-1}$ resolution was used and 512 scans were averaged to improve the signal-to-noise ratio. The range selected for data acquisition was 4000-650 cm^{-1}. Liquid nitrogen was used to keep the detector cool.

Chapter 3

Results

3.1 Zeta Potential

The zeta potential for sol gel and polymer mixture are discussed below. Though the ZetaPlus equipment showed a zero zeta potential for PVP solution, the trend in the solution mixture with decreasing PVP concentration suggests it to have a positive zeta potential. The zero zeta potential shown by the equipment could be accounted for by the high viscosity of the PVP solution.

3.1.1 Molybdenum sol and Molybdenum based Solutions

Zeta Potential calculations were obtained for Molybdenum sol gel and for solutions of molybdenum sol and PVP in the ratio of 1:4, 1:3 and 2:3. The values of zeta potential obtained are shown in table 3.1.

Table 3.1 Zeta Potential of Molybdenum sol and Molybdenum based Solutions

S. No.	Solution Composition	Ratio	Zeta Potential (mV)
1	Molybdenum sol	-	-6.54
2	Molybdenum sol + PVP	1:4	-2.18
3	Molybdenum sol + PVP	1:3	-3.42
4	Molybdenum sol + PVP	2:3	-4.83

3.1.2 Tungsten based Solutions

Table 3.2 Zeta Potential of Tungsten based Solutions

S. No.	Solution Composition	Ratio	Zeta Potential (mV)
1	Tungsten sol + PVP	1:4	7.77
2	Tungsten sol + PVP	1:3	3.4
3	Tungsten sol + PVP	2:3	0.26

Zeta Potential calculations were obtained for solutions of Tungsten sol and PVP in the ratio of 1:4, 1:3 and 2:3. The zeta potential for Tungsten sol gel could not be calculated through the ZetaPlus equipment as the sol gel showed low conductivity. The values of zeta potential obtained are shown in table 3.2

3.2 Morphology of the Ceramics

The obtained nanofibers were thermally treated at 500℃ for 8 hrs to ensure complete decomposition of the polymer and transformation of sol gel into metal oxide. The temperature was chosen because at this temperature MoO_3 exists in a stable polymorph at 480℃[55]. The ceramics obtained from thermal treatment of molybdenum sol gel and PVP mixture under reverse polarity showed a nanotube structure. The diameter of tube increased with increasing concentration of the sol gel in the solution, which was also the case for as spun nanowires. The as spun nanowires for the 2:3 concentration of the mixture, the fibers contained beads. Figure 3.1 shows MoO_3 nanotubes heat treatment of the fibers spun under reverse polarity in the ratio of a) 1:4 b) 2:3.

For the as spun tungsten sol gel PVP nanowires, agglomerates of the sol could be seen on the fibers. The reason for this could be accounted for by the sol was not miscible in the solution and the particles just formed a suspension. Nanogrids were obtained after thermal treatment for both the fibers spun under straight and reverse polarity for the mixture of sol gel and PVP in the ratio of 1:4. No fibers were formed for the sol and PVP solution in the ratio of 2:3 due to low viscosity of the solution. Figure 2.3 and 2.4 shows the nanogrids of WO_3 obtained from fibers spun under straight and reverse polarity respectively.

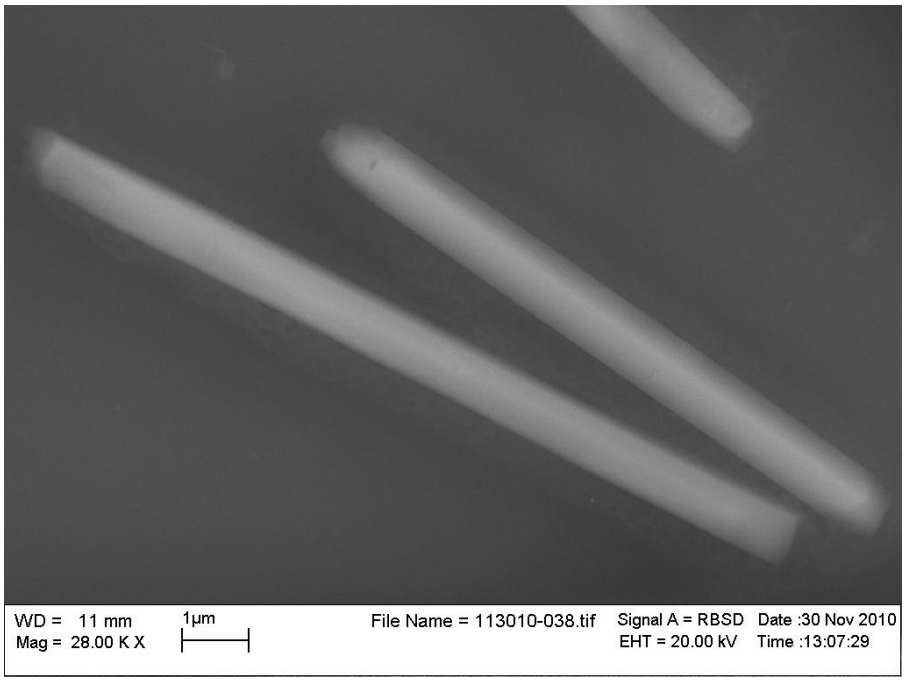

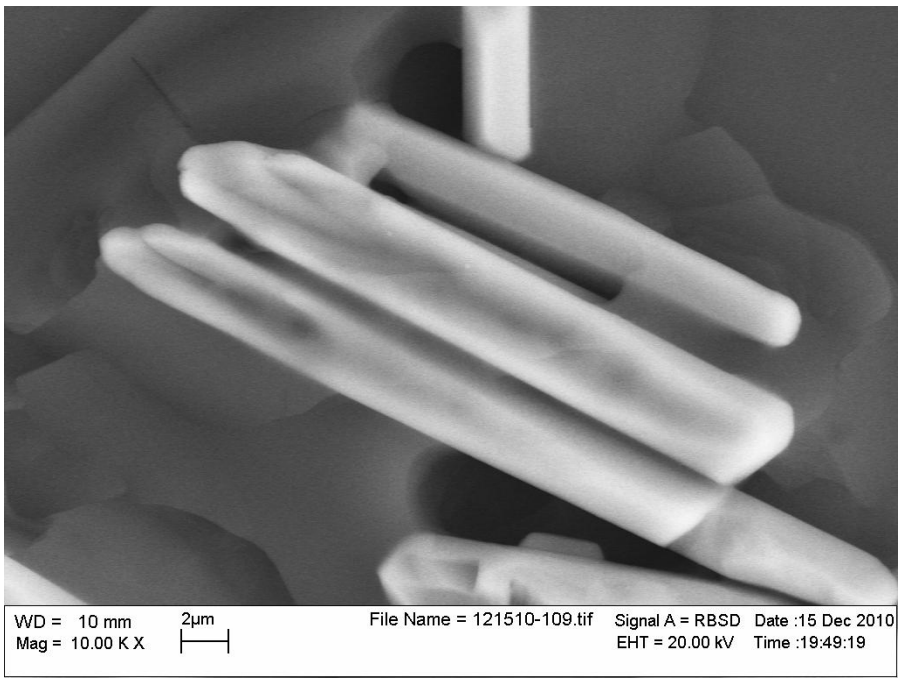

Figure 3.1 MoO_3 Tubes after heat treatment of the fibers spun under reverse polarity in the ratio of a) 1:4 b) 2:3

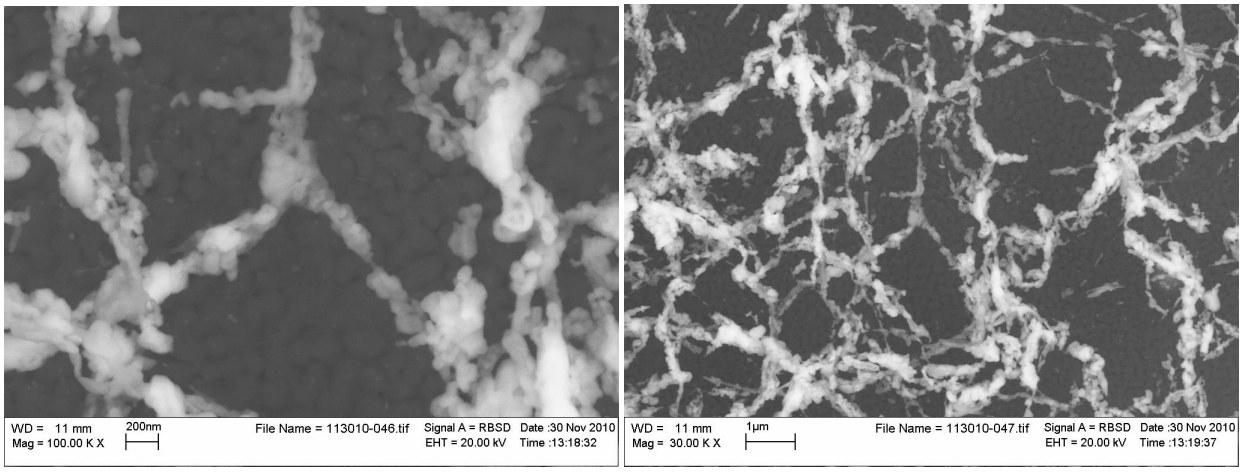

Figure 3.2 WO_3 nanogrids after heat treatment of fibers spun under straight polarity in the ratio of 1:4 a) 100 KX b) 30 KX

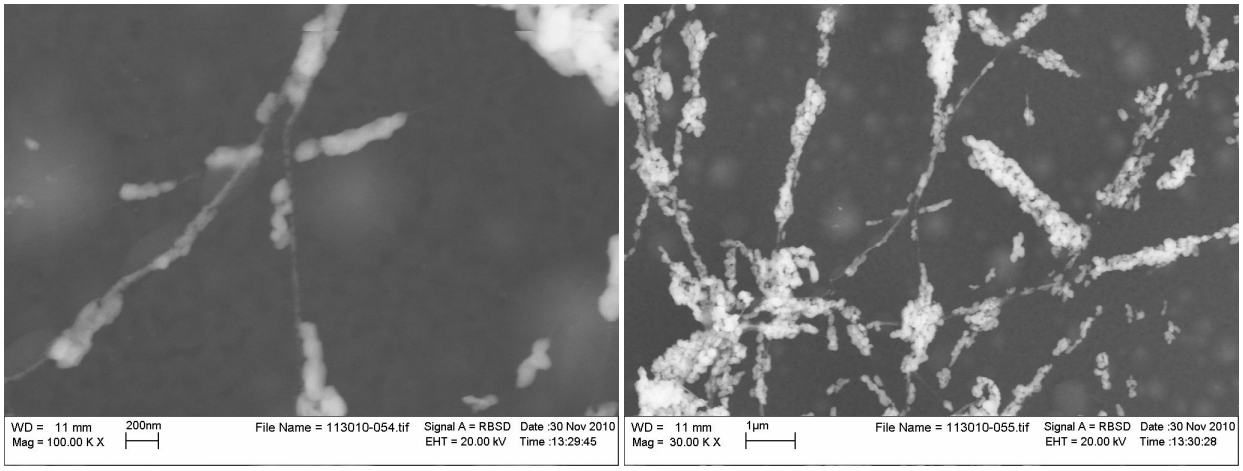

Figure 3.3 WO_3 nanogrids after heat treatment of fibers spun under reverse polarity in the ratio of 1:4 a) 100 KX b) 30 KX

3.3 FTIR Spectrum

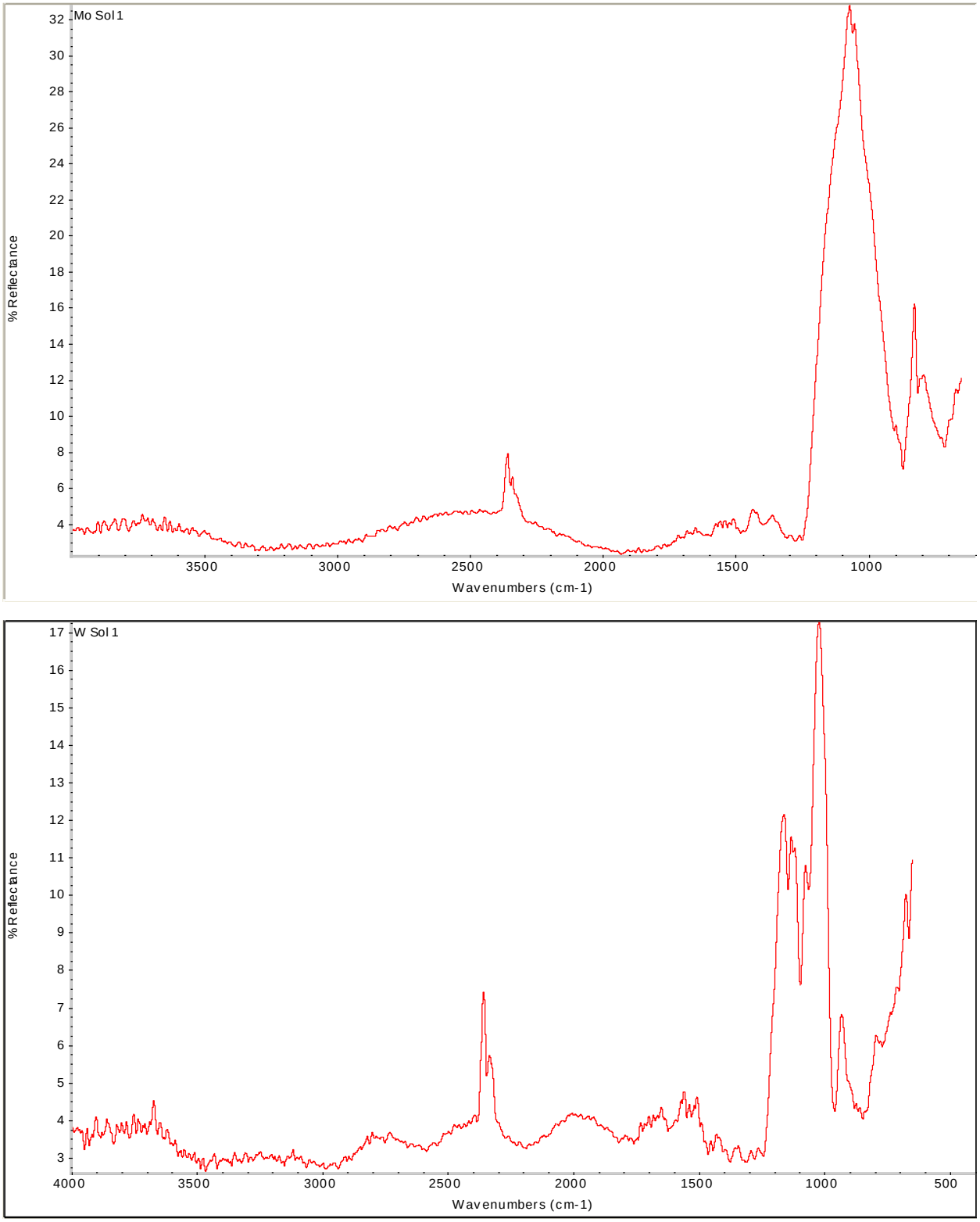

Figure 3.4 FTIR Spectra for a) Molybdenum sol gel b) Tungsten sol gel

The FTIR spectra obtained for Molybdenum shows a peak for Mo-O vibrations at 870 cm^{-1} [56]. There were no other peaks found corresponding to Mo in the spectra.

The FTIR spectra obtained for Tungsten sol gel showed $W=O_t$ [57] vibrations at 961 cm^{-1} which can be due to formation of amorphous WO_3. The spectra also shows vibrations at 1096 cm^{-1} which are the vibrations for W-O-C bonds and could be due to incomplete hydrolysis of the precursor. Figure 3.4 shows the spectra for the Tungsten sol gel.

Chapter 4

Discussion

This work is based on the synthesis of ceramic nanostructures for energy applications by the novel electrospinning process. The nanofibers were successfully spun under straight and reverse polarity. For the same concentration the fiber obtained under reverse polarity had greater diameter than the fibers spun under straight polarity, which is due to lack of coulombic force acting on the sol gel polymer mixture jet [58]. Under reverse polarity of molybdenum sol gel PVP mixture, tubes of MoO_3 were formed after thermal treatment. This can be said to be due to formation of sol on the surface on the as spun fibers. Since the sol gel showed negative zeta potential, the sol gel particles would have been attracted to the surface of the jet while being spun due to a high potential positively charged collector. Nanowires of MoO_3 have been reported earlier when the mixture is spun under straight polarity [59]. Figure 4.1 shows the schematics of MoO_3 nanowires spun under straight and reverse polarity. The formation of nanowires could be the result of embedding of the sol gel particles inside the polymer due to high electrostatic negative charge at the collector. For higher concentration of sol gel in the solution the as spun nanofibers contained beads, the formation of beads resulted from low viscosity of the mixture [4].

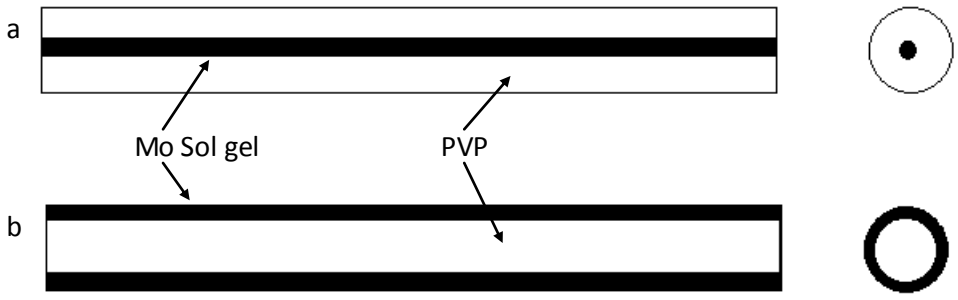

Figure 4.1 schematics showing a) Sol gel Particles embedded inside polymer when spun under straight polarity. b) sol gel particles on surface of polymer when spun under reverse polarity.

For nanofibers spun with tungsten sol gel, the sol particles were agglomerated on the surface of nanofibers, this could be due to immiscibility of the particles in the mixture. The immiscibilility could be said due to formation of amorphous WO_3 in the sol gel. The formation of WO_3 could be accounted for by the vibration peak of $W=O_t$ bond in the FTIR spectra for the Tungsten sol gel. The immiscibility of the particles in the sol lead to the formation of agglomerates on the electrospun fiber. Due to the non conducting nature of amorphous WO_3 a zeta potential for the sol gel couldn't be obtained.

MoO_3 and WO_3 have band gap of 2.82eV [60] and 2.76eV [61]. Due to a low band gap these materials are good candidates to be used in photocatalysis and dye sensitized solar cells, as lower energy will be required for the electrons to get excited from the valence band into condution band. TiO_2 which is currently being used in dye sensitized solar cells and photocatalyst has a much higher band gap of 3.18 eV [61] compared to these materials.

The structures obtained for MoO_3 and WO_3 in this work are very useful in energy applications. For instance nanotubes have high surface-to-volume ration, which is an important factor in increasing photo-energy conversion efficiency [62].

Chapter 5

Conclusion

By employing the electrospinning technique and manipulating its polarity; tailored nanostructures were obtained. The different nanostructured ceramics obtained after thermal treatment could be related to the zeta potential obtained for their solution. Thus by knowing the Zeta potential of the sol gel & polymer mixture to be electrospun, the structure of the nanostructures to be obtained after thermal treatment could be pre known.

Chapter 6

Future work

The behavior could be studied for various other sol gel and polymer solutions and their morphology could be studied. Applying a negative potential could lead to the formation of nanorods and nanotubes for solutions having positive zeta potential and lead to formation of nanogrids for solutions having negative zeta potential.

REFERENCES

1. Prasad A.K.; Study of gas specificity in MoO_3/WO_3 thin film sensors and their arrays; Ph.D. dissertation SUNY Stony Brook 2005
2. A. Formhals: U.S. Patent no. 1,975,504 (1934).
3. Ramakrishna S et al; An Introduction to Electrospinning and Nanofibers; World Scientific 2005
4. Fong H et al.; Beaded nanofibers formed during electrospinning; POLYMER 40 4585-4592 1999
5. Yarin A.L.; Taylor cone and jetting from liquid droplets in electrospinning of nanofibers; JOURNAL OF APPLIED PHYSICS, 90 (9) 4836-4846 2001
6. Regev O et al.; The role of interfacial viscoelasticity in the stabilization of an electrospun jet; POLYMER 51 2611-2620 2010
7. Bazilevsky A et al.; Co-electrospinning of core-shell fibers using a single-nozzle technique; LANGMUIR 23 (5) 2311-2314 2007
8. Kameoka J et al.; A scanning tip electrospinning source for deposition of oriented nanofibers; NANOTECHNOLOGY 14 (10) 1124 2003
9. Jalili et al.; Fundamental parameters affecting electrospinning of PAN nanofibers as uniaxially aligned fibers; JOURNAL OF APPLIED POLYMER SCIENCE, 101 4350-4357 2006
10. Poizot, P; Laruelle, S; Grugeon, S; et al.; Nano-sized transition-metaloxides as negative-electrode materials for lithium-ion batteries; NATURE, 407 (6803): 496-499 SEP 28 2000
11. Zhang, WM; Wu, XL; Hu, JS; et al.; Carbon Coated Fe3O4 Nanospindles as a Superior Anode Material for Lithium-Ion Batteries;ADVANCED FUNCTIONAL MATERIALS, 18 (24): 3941-3946 DEC 22 2008
12. Kim, TW; Park, DH; Lim, ST; et al.; Direct soft-chemical synthesis of chalcogen-doped manganese oxide 1D nanostructures: Influence of chalcogen doping on electrode performance; SMALL, 4 (4): 507-514 APR 2008

13. Ding, N; Liu, SH; Feng, XY; et al.; Hydrothermal Growth and Characterization of Nanostructured Vanadium-Based Oxides;CRYSTAL GROWTH & DESIGN, 9 (4): 1723-1728 APR 2009
14. Bahn, C.S.; Mcgraw, J.M.; et al.; Lithium ion diffusion measurements in high quality $LiCoO_2$ thin-film battery cathodes; MRS symposium proceedings, 575: 71
15. Arai, H and Sakurai,Y; Lithium nickelate with cadmium iodide structure; MRS symposium proceedings, 575: 3
16. Singh, D; Houriet, R; et al.; Pulsed laser deposition and characterization of $LiMn_2O_4$ thin films for applications in Li-ion rechargeable battery systems
17. Jang, Young-Il; Huang, Biying et al.; LiAl*y*Co12*y*O2 (*R*3 – *m*) intercalation cathode for rechargeable lithium batteries; *Journal of The Electrochemical Society,* **146** (3) 862-868 (1999)
18. Wang, Y; Cao, GZ; Developments in nanostructured cathode materials for high-performance lithium-ion batteries;ADVANCED MATERIALS, 20 (12): 2251-2269 JUN 18 2008
19. Kavan, L; Kalbac, M; Zukalova, M; et al.; Lithium storage in nanostructured TiO2 made by hydrothermal growth;CHEMISTRY OF MATERIALS, 16 (3): 477-485 FEB 10 2004
20. Wang, J; Polleux, J; Lim, J; et al.;Pseudocapacitive contributions to electrochemical energy storage in TiO2 (anatase) nanoparticles;JOURNAL OF PHYSICAL CHEMISTRY C, 111 (40): 14925-14931 OCT 11 2007
21. Zukalova, M; Kalbac, M; Kavan, L; et al.; Pseudocapacitive lithium storage in TiO2(B); CHEMISTRY OF MATERIALS, 17 (5): 1248-1255 MAR 8 2005
22. Park, MS; Kang, YM; Dou, SX; et al.;Reduction-free synthesis of carbon-encapsulated SnO2 nanowires and their superiority in electrochemical performance;JOURNAL OF PHYSICAL CHEMISTRY C, 112 (30): 11286-11289 JUL 31 2008
23. Chou, Shulei ; Cheng, Fangyi ; Chen, Jun ; Electrodepostition synthesis and electrochemical properties of nanostructured γ-MnO_2 films; Journal of Power Sources 162 (2006) 727–734
24. Xue, MZ; Fu, ZW; Electrochemical reaction of lithium with nanostructured thin film of antimony trioxide; ELECTROCHEMISTRY COMMUNICATIONS, 8 (8): 1250-1256 AUG 2006
25. Li, YG; Tan, B; Wu, YY; Mesoporous CO3O4 nanowire arrays for lithium ion batteries with high capacity and rate capability; NANO LETTERS, 8 (1): 265-270 JAN 2008

26. Wang, HB; Pan, QM; Zhao, HW; et al.; Fabrication of CuO film with network-like architectures through solution-immersion and their application in lithium ion batteries; JOURNAL OF POWER SOURCES, 167 (1): 206-211 MAY 1 2007
27. Xiang, J. Y. & Tu, J. P.;A comparision of anodically grown CuO nanotube film and Cu_2O film as anodes for lithium ion batteries; J Solid State Electrochem (2008) 12:941–945
28. OREGAN, B; GRATZEL, M; A LOW-COST, HIGH-EFFICIENCY SOLAR-CELL BASED ON DYE-SENSITIZED COLLOIDAL TIO2 FILMS; NATURE, 353 (6346): 737-740 OCT 24 1991
29. Kim, ID; Hong, JM; Lee, BH; et al.; Dye-sensitized solar cells using network structure of electrospun ZnO nanofiber mats; APPLIED PHYSICS LETTERS, 91 (16): Art. No. 163109 OCT 15 2007
30. Ravirajan, P; Peiro, AM; Nazeeruddin, MK; et al.; Hybrid polymer/zinc oxide photovoltaic devices with vertically oriented ZnO nanorods and an amphiphilic molecular interface layer; JOURNAL OF PHYSICAL CHEMISTRY B, 110 (15): 7635-7639 APR 20 2006
31. Olson, DC; Lee, YJ; White, MS; et al.; Effect of ZnO processing on the photovoltage of ZnO/poly(3-hexylthiophene) solar cells; JOURNAL OF PHYSICAL CHEMISTRY C, 112 (26): 9544-9547 JUL 3 2008
32. Bacsa, RR; Dexpert-Ghys, J; Verelst, M; et al.; Synthesis and Structure-Property Correlation in Shape-Controlled ZnO Nanoparticles Prepared by Chemical Vapor Synthesis and their Application in Dye-Sensitized Solar Cells; ADVANCED FUNCTIONAL MATERIALS, 19 (6): 875-886 MAR 24 2009
33. Westermark, K; Rensmo, H; Siegbahn, H; et al.; PES studies of Ru(dcbpyH(2))(2)(NCS)(2) adsorption on nanostructured ZnO for solar cell applications; JOURNAL OF PHYSICAL CHEMISTRY B, 106 (39): 10102-10107 OCT 3 2002
34. Nazeeruddin, MK; Zakeeruddin, SM; Lagref, JJ; et al.; Stepwise assembly of amphiphilic ruthenium sensitizers and their applications in dye-sensitized solar cell; COORDINATION CHEMISTRY REVIEWS, 248 (13-14): 1317-1328 JUL 2004
35. Ravirajan, P; Haque, S.A.; Nanoporous TiO_2 solar cells sensitized with a fluorine-thiophene copolymer; Thin Solid Films 451 –452 (2004) 624–629

36. Zukalova, M; Prochazka, J; Zukal, A; et al.; Organized Mesoporous TiO2 Films Stabilized by Phosphorus: Application for Dye-Sensitized Solar Cells; JOURNAL OF THE ELECTROCHEMICAL SOCIETY, 157 (1): H99-H103 2010
37. Carrette, L; Friedrich, KA; Stimming, U; Fuel cells: Principles, types, fuels, and applications; CHEMPHYSCHEM, 1 (4): 162-193 DEC 15 2000
38. Yoo, Y; Oishi, N, et al. , Development of metal supported thin film SOFC at ICPET/NRCC, CERAMIC ENGINEERING AND SCIENCE PROCEEDINGS, 28 (4): 17-24 2008
39. Suzuki, T; Yamaguchi, T; et al.; Fabrication and optimization of Micro Tubular SOFC for cube type SOFC stacks; CERAMIC ENGINEERING AND SCIENCE PROCEEDINGS, 28 (4): 25-32 2008
40. Yamaguchi, T; El-Toni, A.M.; et al.; Development of fabrication technology for honeycomb-type SOFC with integrated Multi micro cells; CERAMIC ENGINEERING AND SCIENCE PROCEEDINGS, 28 (4): 41-48 2008
41. Appleby, A.J.; Recent Developments in fuel cell materials; MRS SYMPOSIUM PROCEEDINGS, 393 11-14 (1995)
42. Yu, A and Haile, S.M.; Ionic conductivity in $LaCo_{1-x}Mg_xO_{3-\delta}$: a potential cathode material for solid oxide fuel cells, MRS SYMPOSIUM PROCEEDINGS, 393 43-48 (1995)
43. Gustavsson, M; Ekstrom, H; Hanarp, R; et al.; Thin film Pt/TiO2 catalysts for the polymer electrolyte fuel cell; JOURNAL OF POWER SOURCES, 163 (2): 671-678 JAN 1 2007
44. Santos, A.L.; Profeti, D; Electrooxidation of methanol on Pt microparticles dispersed on SnO2 thin films; Electrochimica Acta 50 (2005) 2615–2621
45. Ma, B; Park, J.H.; et al.; Electronic and Ionic conductivity and oxygen diffusion coefficient of the Sr-Fe-Co-O System, MRS SYMPOSIUM PROCEEDINGS, 393 49-54 (1995)
46. Schäfer, G.W.; de Kroon, A.P.; et al.; Order-disorder transitions in gadolinium zirconate: a potential electrolyte material in solid oxide fuel cells; MRS SYMPOSIUM PROCEEDINGS, 393 55-60 (1995)
47. Ishihara, T; Shibayama, T; et al.; Transition metals doped $LaGaO_3$ perovskite fast oxide ion conductor and intermediate temperature solid oxide fuel cells; MRS Symposium Proceedings, 575 283-294 (1999)
48. Blennow, P; Hansen, K.K.; et al.; Niobium doped strontium titanates as SOFC anodes; CERAMIC ENGINEERING AND SCIENCE PROCEEDINGS, 28 (4): 203-214 2008

49. Centi, G; Perathoner, S; The Role of Nanostructure in Improving the Performance of Electrodes for Energy Storage and Conversion; EUROPEAN JOURNAL OF INORGANIC CHEMISTRY, (26): 3851-3878 SEP 2009
50. Kulova, TL; Skundin, AM; Roginskaya, YE; et al.; Lithium intercalation into nanostructured films based on oxides of tin and titanium;RUSSIAN JOURNAL OF ELECTROCHEMISTRY, 40 (4): 432-439 APR 2004
51. Reisner, DE; Salkind, AJ; Strutt, PR; et al.; Nickel hydroxide and other nanophase cathode materials for rechargeable batteries; JOURNAL OF POWER SOURCES, 65 (1-2): 231-233 MAR-APR 1997
52. Centi, G; Perathoner, S; The Role of Nanostructure in Improving the Performance of Electrodes for Energy Storage and Conversion; EUROPEAN JOURNAL OF INORGANIC CHEMISTRY, (26): 3851-3878 SEP 2009
53. Riddick T.M.; Control of colloid stability through zeta potential; Livingston Publishing Company, Vol 1
54. Brookhaven Instruments ZetaPlus Manual
55. Kalyanasundaram K; Biomarker Sensing using Nanostructured Metal oxide sensors; Ph.D. dissertation; SUNY Stony Brook 2007
56. Dong W and Dumn B; Sol-gel synthesis of monolithic molybdenum oxide aerogels and xerogels ; JOURNAL OF MATERIALS CHEMISTRY 8 (3) 665-670 1998
57. Deepa M. et al.; FTIR investigations of solid precursor material for sol-gel deposition of WO_3 based electrochromic films; 35 5313-5318 2000
58. Kilic, A et. al; Effects of polarity on electrospinning process; TEXTILE RESEARCH JOURNAL, 78 (6) 532-539 JUN 2008
59. Kalyanasundaram K;Electrospun single-crystal MoO_3 nanowires for biochemistry sensing probes; JOURMAL OF MATERIALS RESEARCH 21 (11) 2904-2910 2006
60. Hussain Z; Optical and electrochromic properties of heated and anneal MoO_3 thin films; JOURNAL OF MATERIALS RESEARCH; 16 (9) 2695-2708 SEP 2001
61. Lin C.F. et al.; Degradation of 4-chlorophenol in TiO_2, WO_3, SnO_2, TiO_2/WO_3 and TiO_2/SnO_2 systems; JOURNAL OF HAZARDOUS MATERIALS 154 (1-3) 1033-1039 JUN2008

62. Shen G; Fabrication and Characterization of Metal Oxide Nanowire Sensors; RECENT PATENTS ON NANOTECHNOLOGY, 2 160-168 2008